VOLUME 116, NUMBER 18
SEPTEMBER 7, 1994

JOURNAL
OF THE
AMERICAN
CHEMICAL
SOCIETY

Investigation of Medium Effects in a Family of Decarboxylase Antibodies

Theodore M. Tarasow,† Cristina Lewis,‡ and Donald Hilvert*

Contribution from the Departments of Chemistry and Molecular Biology, The Scripps Research Institute, 10666 North Torrey Pines Road, La Jolla, California 92037

Received March 31, 1994®

Abstract: A family of naphthalenedisulfonate-binding antibodies catalyze the decarboxylation of 5-nitro-3-carboxybenzisoxazole, providing a series of structurally similar catalysts for investigating the influence of protein microenvironment on reactivity. Eight representative catalysts and one noncatalytic hapten binder have been characterized in detail to assess their catalytic properties. The Michaelis–Menten parameters, inhibition constants for hapten and product, and thermodynamic activation parameters are reported for each catalyst. The rate accelerations provided by the catalytic antibodies range from 1620 to 23 200. The antibodies display similar affinities for the hapten, substrate, and product, suggesting that binding differences are not the major cause of the variation in catalytic activity. Instead, catalytic efficiency appears to correlate roughly with the hydrophobicity of the antibody active site as judged by fluorescence spectroscopy. Furthermore, five of the catalytic antibodies fit an isokinetic relationship, displaying a wide variation in thermodynamic activation parameters characterized by enthalpy–entropy compensation. The data illustrate the potential of similar proteins to solve a specific chemical problem in slightly different ways and warrant detailed structural investigations to determine the precise combination of hydrogen bonding, electrostatic, and dispersive interactions that constitute medium effects in these related proteins.

Introduction

In the past decade, a large number and variety of catalytic antibodies have been prepared.[1-3] While the synthetic or industrial potential of catalytic antibodies has yet to be fully exploited, these tailored catalysts provide a unique opportunity to study enzyme catalysis and protein structure–function relationships. Certainly, before we can hope to design diverse protein catalysts in a rational and efficient manner, we must fully understand what distinguishes a good catalyst from a bad one. The production of a catalytic antibody by generating monoclonal antibodies against a transition state analog typically results in not one but a family of proteins displaying a range of catalytic efficiencies. A collection of proteins with similar structures but with incremental catalytic competence can provide "snapshots" of progressing catalytic power and may also serve as a crude model for the evolution of a specific catalytic activity. Thus, potentially valuable information can be gained by fully characterizing not just the best catalyst but the entire family of antibodies generated against a single hapten.

We recently described the antibody catalysis of a well-studied decarboxylation reaction as a model system for evaluating the role of medium effects in protein catalysis.[4,5] The decarboxylation of 5-nitro-3-carboxybenzisoxazole (**1**), which proceeds through a charge-delocalized transition state, is notable for its remarkable

† Current address: Nexagen, Inc., 2860 Wilderness Place, Suite 200, Boulder, CO 80301.
‡ Current address: Agouron Pharmaceuticals, Inc., 11099 N. Torrey Pines Rd., La Jolla, CA 92037.
• Abstract published in *Advance ACS Abstracts,* July 15, 1994.
(1) Schultz, P. G.; Lerner, R. A. *Acc. Chem. Res.* **1993**, *26*, 391–395.
(2) Stewart, J. D.; Liotta, L. J.; Benkovic, S. J. *Acc. Chem. Res.* **1993**, *26*, 396.
(3) Hilvert, D. *Acc. Chem. Res.* **1993**, *26*, 552–558.
(4) Lewis, C.; Kramer, T.; Robinson, S.; Hilvert, D. *Science* **1991**, *253*, 1019.
(5) Lewis, C.; Paneth, P.; O'Leary, M. H.; Hilvert, D. *J. Am. Chem. Soc.* **1993**, *115*, 1410.

0002-7863/94/1516-7959$04.50/0

Scheme 1

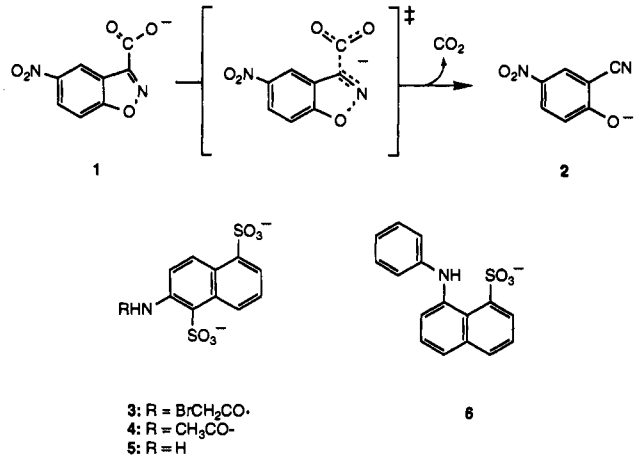

1 2

3: R = $BrCH_2CO$-
4: R = CH_3CO-
5: R = H

6

sensitivity to solvent. The reaction rate is increased dramatically by transfer of the reactant from aqueous media to a dipolar aprotic solvent. For example, the addition of a benzonitrile phase to an aqueous solution of 6-nitro-3-carboxybenzisoxazole enhances the decarboxylation rate by a factor of 10^4, and the reaction rate in neat hexamethylphosphoramide is 10^8-fold greater than that in water.[6-8] Jencks[9] has pointed out that the analogous partitioning of reactants into the less polar medium of a protein binding site is an important catalytic mechanism for enzymes. The rate accelerations that can be attained through effects are potentially enormous and are believed to contribute to the observed rate enhancements afforded by histidine decarboxylase, arginine decarboxylase, and a number of thiamine pyrophosphate-dependent enzymes.[10-12] Our strategy for generating catalysts capable of using medium effects was to create hydrophobic antibody binding pockets with the appropriate size and charge complementarity to the transition state for 5-nitro-3-carboxybenzisoxazole decarboxylation (**1**). The 2-(bromoacetamido)-1,5-naphthalenedisulfonate derivative **3** served well in this capacity.[4] Out of 1200 hybridomas raised against hapten **3**, 25 antibodies (2% of total) were catalytically active. One of the most efficient antibodies (21D8) accelerates the reaction approximately 17 000-fold over the rate in aqueous buffer. Kinetic experiments indicated that 21D8 behaves like a typical enzyme in displaying saturation kinetics and multiple turnovers.[4]

The thermodynamic activation properties of the uncatalyzed and the antibody-catalyzed reactions were characterized in detail. The acceleration in the rate of decarboxylation that is caused by organic solvents has been shown to be due entirely to a lowering of the enthalpy of activation ($\Delta H^{\ddagger}$). The entropy of activation ($\Delta S^{\ddagger}$) is favorable in aqueous buffer and does not change appreciably for the reactions carried out in dipolar aprotic solvents such as acetonitrile.[4,6,7] A favorable $\Delta S^{\ddagger}$ may reflect the liberation of ordered solvent molecules from the substrate as the reaction coordinate is traversed. We observed that the rate acceleration afforded by the catalytic antibody 21D8 is also due to a more favorable activation enthalpy. However, we observed a negative entropic effect relative to the solvent-catalyzed decarboxylation, perhaps reflecting the inability of the protein to relax as the reaction approaches the transition state.[4]

Because the decarboxylation is known to be insensitive to general acid–base catalysis and stereochemical constraints, our results suggest that the 10^4-fold rate acceleration provided by 21D8 can be ascribed almost entirely to medium effects. Fluorescence spectroscopy experiments confirmed that 21D8 has the potential to desolvate the substrate **1**. The fluorescence of hapten derivative **5** (a potent competitive inhibitor of 21D8) is quenched in solution by small solvent-associated molecules. However, no quenching is observed when **5** is bound to the antibody. The fluorophore 1,8-anilinonaphthalenesulfonate (**6**) (1,8-ANS), also a potent competitive inhibitor of catalysis, displays a blue shift in its fluorescence emission spectrum upon binding 21D8. A shift in emission λ_{max} is consistent with movement of the fluorophore from an aqueous environment to an apolar environment. Furthermore, free 1,8-ANS is 2.5 times more fluorescent in D_2O as in H_2O, but no such isotope effect is observed for the bound fluorophore. These results indicate that the binding site of 21D8 is very hydrophobic and is virtually inaccessible to water molecules when occupied.[4] This characterization of the kinetic behavior and active site environment of 21D8 has identified a number of parameters that we have used to analyze other catalysts within the family of monoclonals raised against **3**. We now report a detailed characterization of nine representative monoclonal antibodies from this family that display a wide range in catalytic efficiency.

Experimental Section

5-Nitro-3-carboxybenzisoxazole (**1**),[6] 5-nitrosalicylonitrile (**2**),[6] the hapten precursor (bromoacetamido)-1,5-naphthalenedisulfonate (**3**),[4] and the hapten analogs acetamido-1,5-naphthalenedisulfonate (**4**)[4] were synthesized according to previously published procedures and gave satisfactory spectroscopic data. 2-Aminonaphthalene-1,5-disulfonate (**5**) was purchased from Pfaltz and Bauer. High purity 1-anilinonaphthalene-8-sulfonic acid (**6**) was purchased from Molecular Probes, Inc. and used without further purification. Monoclonal antibodies were prepared as described earlier and purified by ammonium sulfate precipitation, DEAE ion-exchange chromatography, FPLC affinity chromatography on protein G Sepharose, and finally FPLC ion-exchange chromatography (MonoQ HR 10/10).[13]

Kinetic Analyses. Kinetic analyses and UV/vis spectra were obtained using a spectrophotometer equipped with a constant temperature water bath (±0.1 °C). Initial reaction velocities were measured spectrophotometrically in 10 mM Tris-HCl (pH 8.0) by following product formation at 380 nm (ϵ_{380} = 10 800 M^{-1} cm^{-1}). All assays were performed at 20 °C unless indicated otherwise. Uncatalyzed rate constants for the decarboxylation were determined under specific assay conditions and were in agreement with previously reported values.[6] Steady-state kinetic parameters were obtained by fitting initial reaction velocities to the Michaelis–Menten equation. Product inhibition was assessed by Lineweaver–Burke analysis of initial rate data in the presence of varied **2**. Product K_i's were obtained by a replot of the apparent K_m values vs product concentration. Apparent K_i's for the hapten analog **4** were determined at a fixed substrate concentration by fitting initial rate data to the equation for tight-binding inhibition: $v = \{(v_0/2)[\alpha E - I - K_i + [(K_i + \alpha E - I)^2 + 4K_iI]^{1/2}]\}$, where v is the initial rate in the presence of **4**, v_0 is the initial rate in the absence of inhibitor, αE represents the fractional (α) concentration of *functional* antibody binding sites (E), I is the concentration of **4**, and K_i is the apparent inhibition constant.[14] The substrate concentration used in each case was twice the value of the K_m determined for each antibody, and the antibody concentrations ranged from 0.5 to 4.5 μM. Data were fit to the equation describing tight-binding competitive inhibition using the KineTic program from Bio-Kin Ltd. (Madison, WI). Competition ELISA experiments were performed as previously described.[15]

Thermodynamic Activation Parameters. Activation parameters were obtained from linear Eyring plots of $\ln(k_{cat}/T)(h/k)$ vs $1/T$ over the range 9–35 °C, where h and k are Planck's and Boltzmann's constants, respectively. Statistical analysis of the apparent isokinetic relationship was performed using a computer program based on the algorithm

(6) Kemp, D. S.; Paul, K. G. *J. Am. Chem. Soc.* **1975**, *97*, 7305.
(7) Kemp, D. S.; Cox, D. D.; Paul, K. G. *J. Am. Chem. Soc.* **1975**, *97*, 7312.
(8) Casey, M. L.; Kemp, D. S.; Paul, K. G.; Cox, D. D. *J. Org. Chem.* **1973**, *38*, 2294.
(9) Jencks, W. P. *Catalysis in Chemistry and Enzymology*; McGraw-Hill: New York, 1969; pp 228.
(10) O'Leary, M. H.; Piazza, G. J. *Biochemistry* **1981**, *20*, 2743.
(11) Crosby, J.; Stone, R.; Lienhard, G. E. *J. Am. Chem. Soc.* **1970**, *92*, 2891.
(12) Alston, T. A.; Abeles, R. H. *Biochemistry* **1987**, *26*, 4082.
(13) Hilvert, D.; Carpenter, S. H.; Nared, K. D.; Auditor, M.-T. M. *Proc. Natl. Acad. Sci. U.S.A.* **1988**, *85*, 4953–4955.
(14) Williams, J. W.; Morrison, J. F. *Methods Enzymol.* **1979**, *63*, 437.
(15) Friguet, B.; Chaffotte, A. F.; Djavadi-Ohaniance, L.; Goldberg, M. E. *J. Immunol. Methods* **1985**, *77*, 305.

Table 1. Kinetic Parameters and Inhibition Constants Measured at 20 °C for Monoclonal Antibodies Raised against Hapten 3

monoclonal antibody	k_{cat} (min^{-1})	K_m (μM)	K_i[a] (nM) hapten analog 4	K_i (μM) product 2	k_{cat}/K_m (M^{-1} min^{-1})	rate acc k_{cat}/k_{un}
25E10	23.2 ± 0.7	256 ± 15	2.4	14.4 ± 0.1	90 600	23 200
21D8	17.0 ± 0.4	206 ± 12	6.8 ± 0.2 (66.1)[b]	6.4 ± 0.5	82 500	17 000
17E10	16.0 ± 0.7	360 ± 35	3.1	14.5 ± 3.8	44 400	16 000
19F6	13.9 ± 1.0	356 ± 56	4.2 ± 0.4	17.1 ± 2.8	39 000	13 900
32F7	9.95 ± 0.3	100 ± 13	7.4	6.7 ± 2.3	99 500	9950
33D7	6.85 ± 0.3	109 ± 13	12.2	14.5 ± 3.5	63 300	6850
8D2	4.84 ± 0.1	290 ± 21	9.7	4.6 ± 0.5	16 700	4840
27D6	1.6 ± 0.1	119 ± 10	2.1	2.2 ± 1.0	13 600	1620
18F6	NA	NA	(35.3)	NA	NA	0

[a] Standard deviations are less than 1% if not reported. NA = not applicable. [b] Values in parentheses are dissociation constants determined by competitive ELISA.

developed by Exner.[16] The standard deviations of the Arrhenius lines with and without the constraint of a common point of intersection are represented as s_0 and s_{00}, respectively.[16]

Fluorescence Spectroscopy. Fluorescence data were collected using an Aminco-Bowman series 2 Luminescence Spectrometer. The fluorescence spectrum of 1,8-ANS was measured in 10 mM Tris (pH 8.0) by excitation at 372 nm in the presence of a large excess of antibody binding site. Emission maxima were determined by scanning from 400 to 600 nm. Quantum yields were determined by integrating the emission spectra from 400 to 600 nm and comparing the value to that obtained for the free fluorophore in absolute ethanol (quantum yield 0.4).[13] Isotope effects were obtained by comparing the integrated emission spectra from 400 to 700 nm in H_2O to that obtained in D_2O (>99%). All emission spectra were corrected by subtracting the appropriate background spectra. Binding of 1,8-ANS to each antibody was measured fluorometrically using the method of Klotz;[17] increasing concentrations of fluorophore were added to different fixed concentrations of antibody, and the fluorescence was monitored at emission λ_{max}. The data were fit to the following equation, which assumes that all binding sites are identical and noncooperative: $P/XD = K_d/nD(1 - X) + 1/n$, where P is the protein concentration, D is the fluorophore (1,8-ANS) concentration, X represents the fraction of 1,8-ANS bound, K_d is the dissociation constant, and n is the number of binding sites per protein molecule. The fraction of bound fluorophore (X) is equal to F/F_{max}, where F is the fluorescence intensity at a given concentration of protein and 1,8-ANS, and F_{max} is the fluorescence intensity in the presence of excess antibody and varied concentrations of 1,8-ANS (20–1200 nM). In aqueous solution, the fluorescence of free 1,8-ANS is negligible. In the presence of excess antibody, the fluorescence intensity was linearly dependent on the concentration of 1,8-ANS in the range indicated. Thus, a linear plot of P/XD vs $1/(1 - X)D$ yields values of n and K_d.[17,18]

Results and Discussion

From the set of antibodies generated against **3**, eight representative catalysts (out of 25) and one noncatalyst were chosen for detailed mechanistic analyses. All catalytic antibodies displayed saturation kinetics for the decarboxylation of **1**. Although 18F6 was capable of binding the conjugated hapten **3** (see below), this antibody showed no catalytic activity. Fitting the initial rate data for the catalytic antibodies to the Michaelis–Menten equation yielded the kinetic constants shown in Table 1. Although preliminary kinetic data had identified 21D8 as the best catalyst out of 25, detailed kinetic analyses of each purified antibody indicated that 25E10 was in fact more active. Whereas k_{cat} varies by a factor of 14, K_m varies only by a factor of 3.6; k_{cat}/K_m thus displays only a weak correlation with catalytic efficiency. All of the catalytic antibodies demonstrated tight-binding inhibition by the hapten analog **4** (Table 1 and Figure 1). In each case, the concentration of functional catalytic sites (αE) was in agreement with the experimental concentration of antibody combining sites, indicating that the immunoglobulins were physically and kinetically homogeneous and that catalysis was occurring specifically within the antibody binding region. Because 18F6 was not catalytic, a competitive ELISA binding assay was used to determine the dissociation constant for **4**. The value obtained (35 ± 6 nM) was somewhat larger than the apparent inhibition constants for all of the catalytic antibodies but was very similar to the K_d of 66 ± 15 nM measured by competition ELISA for 21D8 and **4**. Thus, the hapten binding affinities are similar and cannot account for any differences in catalytic efficiency (k_{cat}/k_{un}). All of the antibody-catalyzed reactions also displayed product inhibition, with K_i's for the nitrosalicylonitrile **2** in the low micromolar range. Inasmuch as kinetic parameters were measured using initial rates, product inhibition is not likely to influence our measurements of catalytic efficacy.

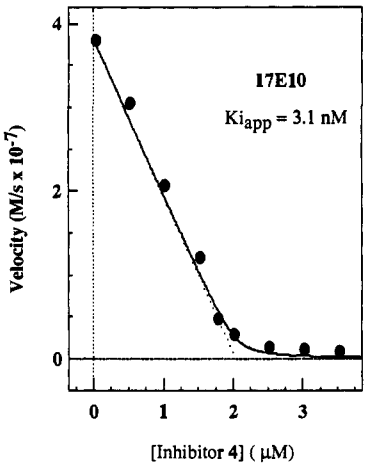

Figure 1. Representative plot of tight-binding inhibition of antibody 17E10 by **4**. Initial rate data measured at increasing concentrations of **4** in the presence of 2.04 μM (binding site) 17E10 and 722 μM **1** ($2K_m$) were fit to the equation for competitive tight-binding inhibition as described in the Experimental Section. The dotted line represents the theoretical fit for a tight-binding competitive inhibitor.

Table 2. Thermodynamic Parameters for Monoclonal Antibodies Raised against Hapten 3

monoclonal antibody	$\Delta H^{\ddagger}$ (kcal/mol)	$\Delta S^{\ddagger}$ (cal/(mol K))	rate acc k_{cat}/k_{un}
25E10	15.6 ± 1.1	−7.6 ± 3.7	23 200
21D8	19.9 ± 0.6	6.6 ± 1.9	17 000
17E10	16.7 ± 0.9	−4.9 ± 3.2	16 000
19F6	12.8 ± 0.9	−17.9 ± 3.0	13 900
32F7	14.9 ± 1.1	−10.3 ± 3.8	9950
33D7	14.7 ± 1.5	−12.8 ± 5.0	5830
8D2	14.3 ± 1.6	−15.2 ± 5.3	4840
27D6	10.3 ± 0.6	−29.2 ± 2.2	1620

Activation parameters for each of the catalysts were determined by Eyring analysis of the temperature dependence of k_{cat} for each reaction (Table 2). The most striking observation is the large range in the entropy of activation (35.8 eu), from a favorable

(16) Exner, O. *Prog. Org. Chem.* **1973**, *10*, 411.
(17) Klotz, I. M.; Walker, F. M.; Pivan, R. B. *J. Am. Chem. Soc.* **1946**, *68*, 1486.
(18) Christian, S. T.; Janetzko, R. *Arch. Biochem. Biophys.* **1971**, *145*, 169.

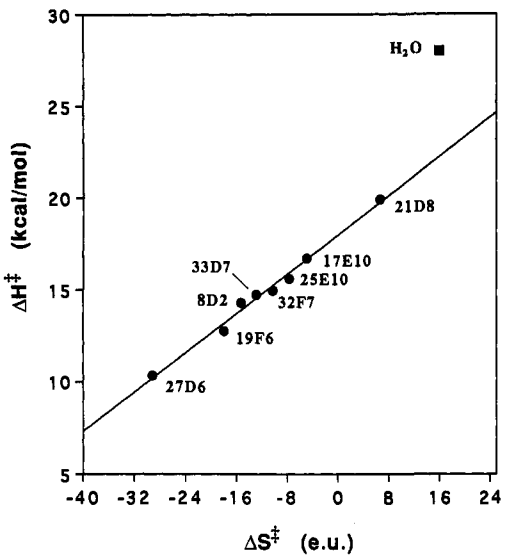

Figure 2. Linear relationship between $\Delta H^{\ddagger}$ and $\Delta S^{\ddagger}$ for the decarboxylation of 5-nitro-3-carboxybenzisoxazole catalyzed by antibodies (●) and in water (■). The antibody-catalyzed thermodynamic activation parameters were fit using linear regression, yielding a straight line with slope = 0.266 and correlation coefficient = 0.994.

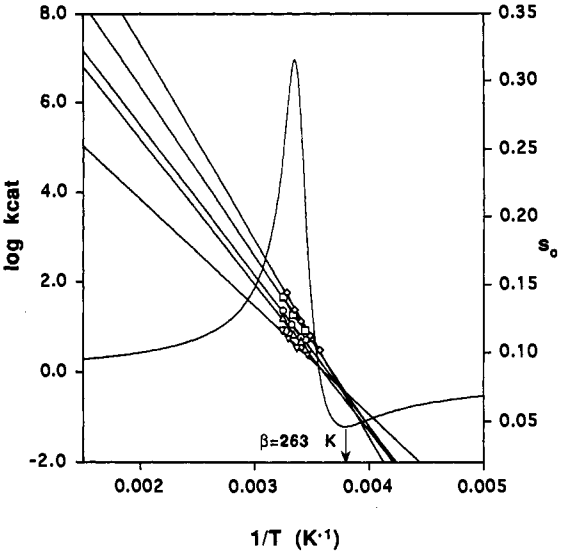

Figure 3. Isokinetic relationship for the decarboxylation of 5-nitro-3-carboxybenzisoxazole by catalytic antibodies 21D8 (◇), 17E10 (□), 33D7 (○), 8D2 (△), and 27D6 (▽). The standard deviation of the Arrhenius lines with the constraint of a common point of intersection (s_0) was determined by the method of Exner[12,26] (curved line).

positive $\Delta S^{\ddagger}$ for one of the most efficient catalysts to large negative values for the worst catalysts. The relationship between the entropy and enthalpy of activation for these catalysts is particularly intriguing. One of the best catalysts (21D8) displays the most favorable $\Delta S^{\ddagger}$ (+6.6 eu) and the least favorable $\Delta H^{\ddagger}$ (19.9 kcal/mol), whereas the worst catalyst (27D6) displays the least favorable $\Delta S^{\ddagger}$ (–29.2 eu) and the most favorable $\Delta H^{\ddagger}$ (10.4 kcal/mol).

Apparent compensation between enthalpy and entropy of activation is not limited to these two antibodies but is true for several of the catalysts. A plot of $\Delta H^{\ddagger}$ vs $\Delta S^{\ddagger}$ yields a straight line (correlation coefficient = 0.994) as shown in Figure 2, suggesting that the entire family of catalysts displays compensation.[19-21] While linearity in a ΔH–ΔS plot may arise from experimental or statistical error,[21] deviation from linearity implies a different chemical mechanism.[16] It is noteworthy that the thermodynamic activation parameters for the decarboxylation of 5-nitro-3-carboxybenzisoxazole in water lie considerably off the line generated by the antibody-catalyzed reactions, underscoring potential mechanistic differences between the aqueous and the protein-catalyzed decarboxylations.

A more rigorous statistical analysis of entropy–enthalpy compensation was performed according to the method of Exner.[16,31] This approach permits the identification of the common point of intersection for a set of Arrhenius plots from which the isokinetic temperature (the temperature at which all rate constants are equal) can be determined. In order for an isokinetic relationship to be statistically valid, the constrained standard deviation obtained with a common point of intersection (s_0) must be less than the unconstrained standard deviation of the free Arrhenius lines (s_{00}).[16,31] Our data indicate that the Arrhenius lines for five of the antibodies (21D8, 17E10, 33D7, 8D2, and 27D6) intersect at a common point where $s_0 < s_{00}$. These results provide unequivocal evidence for the existence of a chemical compensation effect for these catalytic antibodies (Figure 3). The isokinetic temperature (β) determined from the statistical analysis is 263 K, which is very similar to the β value of 264 K calculated from the slope of the $\Delta H^{\ddagger}$–$\Delta S^{\ddagger}$ plot shown in Figure 2. Despite the linear $\Delta H^{\ddagger}$–$\Delta S^{\ddagger}$ plot for all monoclonal antibodies, the more rigorous statistical analysis indicated that three of the antibodies, including the best catalyst 25E10, did not fulfill the criteria for compensation.

It is clearly not a simple matter to identify the molecular phenomena responsible for changes in the enthalpy and entropy of activation for this reaction. The precise reasons for an isokinetic relationship have been a source of great interest and debate in the literature, and several theories have been proposed. Lumry has argued that the source of compensation lies in the perturbation of water structure surrounding proteins and small molecules.[19] On the other hand, Eftink has pointed out that a perturbation in the state of surrounding water molecules is triggered by a ligand-induced change in the state of the protein and it is the protein dynamics that are the source of the compensation phenomena.[32] While the exact molecular explanation for compensation of entropy–enthalpy activation parameters remains a source of debate, it is clear that the existence of a valid isokinetic relationship is a necessary condition for a linear free energy relationship.[33] That is, a related series of reactions with a common mechanism would be expected to display entropy–enthalpy compensation.[29] Thus, our data indicate that five of the antibody catalysts share

(19) Lumry, R.; Rajender, S. *Biopolymers* **1970**, *9*, 1125.
(20) Hammes, G. G. *Nature* **1964**, *204*, 342.
(21) Although a survey of the literature indicates that a linear ΔH–ΔS plot is commonly used to demonstrate entropy–enthalpy compensation,[22-27] several authors have pointed out that linearity could arise from either experimental or statistical error, inasmuch as both ΔH and ΔS are evaluated from the same data set.[28-30] Statistically unobjectionable criteria for compensation include the linear dependence of $\Delta H^{\ddagger}$ and $\Delta G^{\ddagger}$ [28] and the linear dependence of log k values measured at two different temperatures.[29] Pedersen[30] and Exner[16] have argued that an isokinetic relationship exists if all log k_{cal} vs $1/T$ plots intersect at a common point.
(22) Inoue, Y.; Liu, Y.; Tong, L.-H.; Shen, B.-J.; Jin, D.-S. *J. Am. Chem. Soc.* **1993**, *115*, 10637.
(23) Cole, S. J.; Curthoys, G. C.; Magnusson, E. A. *J. Am. Chem. Soc.* **1970**, *92*, 2991.
(24) Ito, W.; Iba, Y.; Kurosawa, Y. *J. Biol. Chem.* **1993**, *268*, 16639.
(25) Murakami, K.; Sano, T.; Tsuchie, S.; Yasunaga, T. *Biophys. Chem.* **1985**, *21*, 127.
(26) Wang, I.-C.; Braid, P. E. *Biochim. Biophys. Acta* **1977**, *481*, 515.
(27) Harrison, R. K.; Stein, R. L. *J. Am. Chem. Soc.* **1992**, *114*, 3464.
(28) Krug, R. R.; Hunter, W. G.; Grieger, R. A. *Nature* **1976**, *261*, 566.
(29) Exner, O. *Nature* **1964**, *201*, 488.
(30) Pedersen, R. C. *J. Org. Chem.* **1964**, *29*, 3133.
(31) Dorovska-Taran, V.; Momtcheva, R.; Gulubova, N.; Martinek, K. *Biochim. Biophys. Acta* **1982**, *702*, 37.
(32) Eftink, M. R.; Anusiem, A. C.; Biltonen, R. L. *Biochemistry* **1983**, *22*, 3884.
(33) Connors, K. A. *Chemical Kinetics: The Study of Reaction Rates in Solution*; VCH Publishers, Inc.: New York, 1990; pp 368–371.

Table 3. Fluorescence Data for Monoclonal Antibodies Raised against Hapten 3

monoclonal antibody	K_d (nM) ANS	no. of sites[a]	λ (nm)	quantum yield (%)	isotope effect	rate acc k_{cat}/k_{un}
25E10	323	1.86	464	0.49	1.29	23 200
21D8	136	1.90	455	1.1	1.07	17 000
17E10	297	1.97	455	0.91	1.04	16 000
19F6	47.7	1.76	455	0.91	1.07	13 900
32F7	150	1.71	461	0.64	1.33	9950
33D7	160	2.37	454	1.1	1.04	5830
8D2	3033	1.86	468	0.43	1.61	4840
27D6	1088	0.83	472	0.25	2.39	1620
18F6	406	0.41	464	0.75	1.11	0

[a] Number of binding sites per IgG molecule.

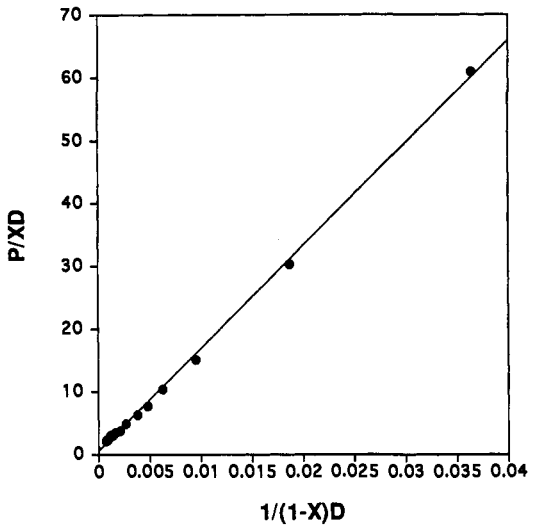

Figure 4. Representative Klotz plot for binding of **6** to antibody 8D2, according to the equation described in the Experimental Section.

a common mechanism, but it is unclear whether or not the statistically excluded proteins catalyze the reaction by alternative pathways.

To further investigate possible mechanistic differences between the catalytic antibodies, the active site microenvironment of each antibody was examined by fluorescence spectroscopy using the probe 1,8-ANS (**6**). Previous studies showed that this environmentally sensitive fluorophore is a potent competitive inhibitor of 21D8, presumably due to the similarity in structure between **3** and **6**.[4] The affinity of 1,8-ANS for each of the antibodies (including the noncatalyst 18F6) was determined using the method of Klotz.[17,18] 1,8-ANS bound rather tightly to all antibodies, with K_d's ranging from 48 nM to 3 μM (Table 3). A representative Klotz plot is shown in Figure 4. All but two of the antibodies displayed approximately two binding sites for **6** per antibody molecule, consistent with binding of the fluorophore to the hapten binding pocket. In contrast, the number of binding sites measured for 27D6 and 18F6 were $n = 0.8$ and 0.4, respectively. Such low binding stoichiometries suggest that 1,8-ANS is binding nonspecifically to these antibodies. In the absence of information about the active site microenvironment of these proteins, we can only speculate as to their catalytic incompetence. Model studies suggest that a hydrophilic active site that is capable of hydrogen bonding to the carboxylate anion would be an inferior catalyst.[6-8]

The emission maxima and quantum yields for bound 1,8-ANS reflect active-site hydrophobicity (Table 3). Those antibodies that bind 1,8-ANS and result in the greatest blue shift in emission λ_{max} (to ~455 nm) and the highest quantum yields (~1) would be expected to have more hydrophobic active sites than the antibodies with lower quantum yields and higher λ_{max} values. In addition, because 1,8-ANS is 2.5 times more fluorescent in D_2O than in H_2O, measurement of the ability of D_2O to enhance the fluorescence of the bound fluorophore provides a direct estimate of the solvent accessibility to the binding pocket. Thus, an isotope effect of 1.0 indicates that D_2O is unable to enhance the fluorescence of the bound fluorophore, suggesting that solvent molecules have limited access to the occupied active site. Conversely, an isotope effect of 2.5 indicates that D_2O is fully accessible to the bound fluorophore. Not surprisingly, the antibody–fluorophore complexes displaying the lowest emission maxima and the greatest quantum yield also display very small isotope effects, indicating that these antibody binding pockets are very hydrophobic and have the potential to exclude solvent from the occupied binding site. With the exceptions of 33D7 and 25E10, the trend in active site hydrophobicity and desolvation potential correlates with catalytic efficiency.

Although all of the antibodies are expected to partition the substrate from aqueous buffer into a hydrophobic binding pocket, the inconsistencies we observe in the fluorescence data may simply represent differences in the way each antibody binds the substrate and the fluorophore probe 1,8-ANS. Alternatively, our data may reflect small mechanistic perturbations inherent in even relatively simple enzymatic catalytic mechanisms. The three antibodies 21D8, 33D7, and 25E10 may illustrate multiple responses to a common catalytic challenge. The catalyst 21D8 has an apolar binding site microenvironment that is quite favorable for promoting the decarboxylation, and this catalyst is among the five antibodies that display an isokinetic relationship. The antibody 33D7 is also part of the isokinetic group and is significantly less active than 21D8, in spite of the fact that it apparently possesses a catalytically favorable hydrophobic binding site. Perhaps most intriguing is the antibody 25E10, which has a greater rate enhancement than 21D8 but appears to have a more polar, solvent-accessible binding site. This paradox may reflect subtle differences in the catalytic mechanism of 25E10 and possibly explain its exclusion from the isokinetic group. The ability of structurally similar proteins to solve the same chemical problem in slightly different ways warrants further investigation of their structure–function relationships. Such studies may help to unravel the complex interplay of hydrogen bonding, electrostatic interactions, and dispersive forces that constitutes medium effects.

In summary, the characterization of a family of antibodies that catalyze a simple, well-defined model reaction suggests that catalysis of this decarboxylation is primarily dependent on active-site microenvironment rather than binding affinity for hapten, substrate, or product. These results are consistent with the rate acceleration of carboxybenzisoxazole decarboxylation observed in dipolar aprotic solvents. However, unlike the solvent-accelerated reactions, the protein-catalyzed decarboxylations display a wide range in entropy of activation. Our analysis of the thermodynamic activation parameters demonstrates that five of the catalytic antibodies display statistically valid entropy–enthalpy compensation. Mechanistic and kinetic characterizations of families of catalysts are a critical first step toward the ultimate goal of relating protein structure with function. Determination of the structure of representative catalysts will likely provide further insight into the use of medium effects as an enzymatic catalytic strategy.

Acknowledgment. This research was supported in part by Faculty Research Award FRA-369 from the American Cancer Society, Grant GM38273 from the National Institutes of Health (D.H.), and a fellowship from the Jane Coffin Childs Memorial Fund for Medical Research (C.L.). We gratefully acknowledge the assistance of Suzanne Robinson and Rich Daniels for antibody preparation and purification. In addition, we also thank Tom Macke for writing the computer program for the statistical analysis of thermodynamic data and Petr Kuzmic for helpful discussions about specific adaptations of KineTic.